INTENSITY MEASUREMENT OF TRAVELLING WAVES IN WEBS USING LASER-DOPPLER SENSORS

By

KRISHNA J VEDULA

Bachelor of Technology

Bapatla Engineering College

Bapatla, India

1992

Submitted to the Faculty of the
Graduate College of the
Oklahoma State University
in partial fulfillment of
the requirements for
the Degree of
MASTER OF SCIENCE

OKLAHOMA STATE UNIVERSITY

INTENSITY MEASUREMENT OF TRAVELLING WAVES
IN WEBS USING LASER-DOPPLER SENSORS

Thesis Approved:

Thesis Adviser

Dean of the Graduate College

ACKNOWLEDGEMENTS

I take this opportunity to express my deepest gratitude and respect towards Dr. Moretti, without whose help and consistant guidance this project would not have been at the stage it is now. I thank him for his timely suggestions. I owe my thanks and respect to Dr. Chang for his co-operation and constant help throughout the completion of this project. I like to thank Dr. Price and Dr. Lowery for serving on my graduate committe.

I would like to thank the Web Handling Research Center for providing me with financial support.

I would also like to express my thanks to my parents, brothers and sisters, whose love and effection made me feel strong and continue my studies.

TABLE OF CONTENTS

Chapter Page

LIST OF TABLES

LIST OF FIGURES

LIST OF SYMBOLS

A	Amplitude
c	Wave speed
c_a	Added mass coefficient
C_i	Amplitude coefficients in the general solution
D	bending stiffness of the beam or plate
e	Base of natural logarithms
F	Force
f	Frequency
i	imaginary root of -1
k	Wave number
M	Bending moment
m	Mass per unit length of string or beam;
	mass per unit area of membrane or plate
m_a	Added mass of air
m_w	Mass per unit area of the web
P	Power flow
p	Pressure perturbation
Q	Shear force
R	Auto or cross correlation function
S	Cross power spectrum
t	Time

T	Tension in the web
u,w	Displacements in x and z-direction respectively
$\dot{w}$	Velocity in z-direction
W	Fourier tranform of transverse displacement
Δx	Distance between measuring points
θ	Angular displacement
λ	Wave length
ρ_a	Density of the surrounding air
ρ_w	Areal density of the web
τ	Time lag
ω	Angular frequency
$\langle\ \rangle_t$	Time-averaged quantity
*	Indicates complex conjugate

CHAPTER 1

INTRODUCTION

High speed production of webs involves high operating speeds of production machinery. These machines are sources of vibrations, hence web flutter, because of the high velocities of both web (3000 fpm to 4000 fpm) and air (6000 fpm to 10000 fpm), and make it necessary to probe into the sources of the vibrations, their travel, and the mechanisms by which they can damage the web. Possible methods of reducing the flutter have to be investigated at the design stage. For web-borne vibrations, power flow measurements and data analysis are needed for identifying the directions of vibration propagation and their source locations.

To determine power flow, we can measure the structural wave intensity which indicates the direction and magnitude of power flux. Wave intensity is the energy flux or power flow transmitted along waves in air, liquids or structures. Based on the characteristics of the structure (thickness, shape, discontinuities, etc.), different types of waves can propagate within the structure. The typical requirements, and consequently the information, that the analysis or measurement should provide are:

the location of sources of vibration.

the identification of the paths of vibration energy flow.

the identification of regions of energy absorption.

The availability of non contact measurement techniques like Laser vibrometers, makes it possible to measure the basic wave characteristics in webs without altering the dynamic behavior of the web. A complete understanding of the wave properties is required before computing the power flow in the web, and this study focuses on measuring the basic wave properties and computing the power flow using the intensity

algorithms. The objective of this thesis is to test and demonstrate the use of intensity algorithms.

1.1. Literature Review

The development of a method to determine the power flow was initiated by Noiseux [12], who derived expressions for the intensity flow through a unit length cross section of a thin plate. He simplified the equation for governing the flexural waves by making simple assumptions to arrive at a realistic measurable quantity. His free field condition assumptions restrict the measurements near any source or boundary. He showed that structural intensity due to the out-of-plane motion is based on three components related to the shear force, the bending moment and the twisting moment.

Later, Pavic [13] applied finite-difference approximations for the governing flexural equations and showed that an array of four transducers is necessary for the measurement of one-dimensional wave intensity, to include the near-field effects as well. He suggested an arrangement of eight transducers to obtain the estimates of spatial derivatives in the governing equation for a two dimensional structure. He also suggested that in case of a sinusoidal motion in one-dimension a two point measurement is adequate. The methods advised by these two authors utilize measurements made in the time domain, and only address the structural intensity associated with out-of-plane vibration.

One of the first measurements of the structural intensity propagated by both out-of-plane and in-plane waves has been presented by Verheij [22]. He showed that the measurement of the power flow could be simplified by transforming to the frequency domain and using cross-power spectra to make the measurements. While his technique for measuring the intensity associated with the out-of-plane waves is the same as the one used by Pavic, for the in-plane components of the intensity, an accelerator configuration

is used which measures both the longitudinal and torsional accelerations and eliminates the out-of-plane component of acceleration.

Most of the experiments have been performed on generally ideal structures, like beams(1-D) or plates(2-D), and their behavior is similar to infinite beams and plates or simulated conditions. Cuscheri [4] has performed experiments on an aircraft fuselage and demonstrated the suitability of his approach for measuring structural intensity on a real structure. He used an array of four transducers and he suggested methods to compensate for the phase error of the measurements. He concluded that the method proved to be inefficient at higher frequency ranges, which can be attributed to errors in measurements associated with the far-field assumption.

Verheij [23], measured the structure-borne sound energy flow through pipes and he successfully demonstrated the methods of transmission path ranking. He found a strong analogy with the two-microphone cross-spectral density for air-borne sound intensity methods. He conducted experiments on lightly damped pipe sections of a cooling water circuit, and outlined some procedures for error analysis. He used a set of four accelerometers for measurement purposes. He concluded that high quality instrumentation is needed in a practical situation because of the highly reactive fields that can be expected.

Another attempt to make measurements on complex structures, like airplanes, was by McGary [10], who suggested improved methods to include near-field effects as well. He followed the ideas of Pavic, employing central finite-difference approximations to the governing equation to estimate the power flow in the frequency domain. This method requires a set of 5 transducers to estimate power flow in a one-dimensional structure and 13 for a two-dimensional structure. He performed a comparative study of the near-field and far-field measurement techniques and studied the performance of the far-field method, near simple sources and boundary conditions. In his work, he concluded that the simulation of free-field measurement near the boundaries seemed to indicate that the

intensity is flowing, actually, in the wrong direction. Furthermore, he demonstrated that this type of error is not necessarily restricted to lower frequency ranges and can occur in frequency ranges where the power flow is relatively large and stable.

He suggested that the free-field approach may be quite useful for obtaining estimates of power flow in situations where there are no sources nearby, or in situations where the properties of the structure do not change in the vicinity of the measurement probe. He expressed the idea that many of the serious near-field errors inherent in the method can be suppressed by increasing the spacing between the measuring points, but this is a compromise since the increase in the accelerometer gap increases the finite-difference errors.

An attempt to distinguish the different components that contribute to the total energy flow was done by Downing [6]. He adapted the method suggested by McGary, and compared the near and far-field measurements. He demonstrated the component breakdown of shear and bending terms in the energy flow for a simple case of an excited beam.

Applying Noiseux's far field measurement of vibrational energy flow involves the use of two closely spaced transducers and a finite-difference approximation. The general trend is to use two accelerometers, but, unfortunately, they tend to alter the dynamic behavior of the vibrating structure. Additionally, because of the need for rigid attachment, accelerometers restrict the ability to easily map the structural energy flow paths over a surface. Also, the mass of the accelerometer was found to have a big influence on the vibration of the structure itself. These considerations which hindered the practical implementation of structural measurements to date, are overcome by adapting techniques now used in laser vibrometry. These techniques facilitate the intensity mapping and avoid the problem of interference with the structural response.

McDevitt et.al. [9], have used a two-channel laser vibrometer (TCV) in which two laser beams activated by the same laser having their beams focused at two closely spaced

points on the surface, replacing the two accelerometers used in conventional far-field measurement. They used a reverberant beam in measuring the flexural intensity in a beam vibrating a resonant frequency. They observed that their method is not phase sensitive and is not subject to phase errors.

To adapt one particular method, of those stated above, one has to consider the structural properties. In the case of a thick plate structure, in-plane motion and the effects of shear deformation and rotary inertia must be taken into account. In this case, the structural intensity has components which are associated with shear force and twisting moments due to the out-of-plane motion, and other components associated with the longitudinal and shear forces due to the in-plane motion.

But, for the case of a thin plate structure, in-plane stresses and deflection can be neglected, and only the out-of-plane deflection of the neutral plane needs to be considered. In this case the structural intensity has components which are associated with the shear force, the bending moment and the twisting moment. The structural intensity at any point on the plate is given by the sum of these three components.

Although there have been methods which show how to include the near-field effects, many studies of power flow continue to use Noiseux's free-field method because of its simplicity. Since, this method uses a finite-difference approximation of the first order in the far-field, a two-point measurement is sufficient. The measurement of structural intensity using a high-order finite-difference approximation is difficult. It has been pointed out that the method is very sensitive to measurement errors: amplitude error, phase resolution positioning of each transducer, phase mismatch, relative positioning between sensors, and the influence of the reactive field on the measurement. For low-order finite-difference approximations, measurement errors are not so important. Most experiments carried out in the past used the expression for the intensity measurement in the far-field, away from discontinuities.

1.2. Research Objective

The object of the study is two-fold: the first part is to distinguish between traveling and standing waves, and the second part is to devise a method to measure the intensity flow of traveling waves in webs. The properties of a traveling wave are constant amplitude at any measurement location, and phase difference between the measurement points. A two-point measurement is sufficient to confirm the existence of a traveling wave. On the other hand, for a standing wave, the amplitude is a function of the distance from the fixed end, and several data points are needed to define the wave pattern. The location of the nodal points can be confirmed from the zero amplitude at those locations. The phase difference for any two points in a pure standing wave is either 0 or 180 degrees, and this information can be used for confirmation.

To measure the intensity flow of traveling waves in webs, when a standing wave might also be present, either a multi-point measurement, or a two-point measurement with added information regarding the governing equation is required. To make use of a two-point measurement method, assumptions have been made regarding the governing equation, and the proximity of boundaries and discontinuities is avoided.

Our study of web flutter and its intensity measurements is done by artificially exciting the web with an acoustical system, and observing the basic phenomenon occurring. Simple boundary conditions and sources of excitation are used to test the theory and develop an algorithm, which can be later applied to more complex disturbing sources. Chapter 2 describes the basic theories in determining the intensity flow in simple structural elements, such as strings, beams, and plates. It also develops the expressions for transforming the time domain signal to frequency domain. The experimental setup and method of experimentation are given in Chapter 3. The methods to calculate the fundamental wave characteristics are given in this chapter along with some sample

calculations. The next step is to compare the results and this is done in Chapter 4 where the experimentally measured intensity flow is compared with theory. Conclusions and suggestions for future work are presented in Chapter 5.

CHAPTER 2

BASIC THEORIES

Wave Intensity, defined as the energy flux transmitted, can be very useful since it is a vector quantity. The acoustic intensity technique makes it possible to determine the sound power level of a noise source, to find the direction of sound propagation and to find the location of sound source. By applying intensity method to a taut string or membrane, it is possible to distinguish between traveling and standing waves.

This chapter includes a review of the fundamentals of power flow in different structural elements such as a string, membrane, beam and a plate. This discussion results in a method to measure the vibrational intensity in different structural elements. Mechanical power flow, caused by a point source, is the time averaged rate of work done by that force. This can be used in defining the intensity in different structural elements.

2.1 Acoustical intensity

Sound intensity is defined as the time averaged product of the pressure perturbations and the velocity of the vibrating air. Rasmussen [17, 18], has given a detailed study of the theory and measurement of sound intensity and source location. Gade [7] has given the instrumentation for determining the sound power from sound intensity measurements.

$$\langle P \rangle_t = \langle pu \rangle_t \qquad 2.1$$

Sound pressure can easily be measured by the use of microphones, but it is difficult to measure the instantaneous velocity of air. However, if we consider a plane wave where all the particles on a plane normal to the direction of propagation of the wave are moving together, the particle velocity can be related to the pressure gradient with the linearized Euler's equation

$$\rho \frac{\partial u}{\partial t} = -\frac{\partial p}{\partial x} \qquad 2.2$$

The velocity of air can be obtained by integrating the pressure gradient.

$$u(t) = -\frac{1}{\rho}\int_0^t \frac{\partial p}{\partial x} d\tau \qquad 2.3$$

Then power flow becomes

$$\langle P \rangle_t = -\frac{1}{\rho}\left\langle p \int_0^t \left(\frac{\partial p}{\partial x}\right) d\tau \right\rangle_t \qquad 2.4$$

Applying finite-difference approximation velocity can be rewritten as

$$u(t) = -\frac{1}{\rho}\int_0^t \frac{p_2 - p_1}{\Delta x} d\tau \qquad 2.5$$

Hence the sound power flow along the x-direction becomes

$$\langle P \rangle_t = -\frac{1}{\rho}\left\langle \frac{(p_1 + p_2)\int_0^t (p_2 - p_1) d\tau}{2\Delta x} \right\rangle_t \qquad 2.6$$

For a standing wave this yields a zero intensity, and for a pure harmonic wave, $p = p_0 \,\mathrm{Re}[e^{i(kx-\omega t)}]$ the exact value of the power flow will turn out to be

$$\langle P \rangle_t = \frac{p_0^{\,2}}{2\rho c} \qquad 2.7$$

2.2. Vibration intensity on a taut string or a membrane

Waves, in a string or membrane, are transverse waves where each element oscillates in the plane normal to the direction of propagation. Hence, the intensity can be defined as the product of the transverse component of tension and the oscillating velocity of an element.

The oscillating velocity is $\frac{\partial w}{\partial t}$ and the transverse component of tension is $\frac{\partial w}{\partial x}$. Then, the time averaged power flow in the x-direction is

$$\langle P \rangle_t = -T\left\langle \left(\frac{\partial w}{\partial x}\right)\left(\frac{\partial w}{\partial t}\right)\right\rangle_t \qquad 2.8$$

Applying finite-difference approximations, the expression for the average power flow on a taut string or membrane becomes

$$\langle P \rangle_t = -T\left\langle \frac{(w_2 - w_1)}{\Delta x}\,\frac{(\dot{w}_2 + \dot{w}_1)}{2}\right\rangle_t \qquad 2.9$$

The cross-correlation of two signals is defined as

$$R_{ab}(\tau) = \frac{1}{T_p}\int_0^{T_p} a(t).b(t+\tau)dt \qquad 2.10$$

Hence the power flow equation becomes

$$\langle P \rangle_t = -\frac{T}{2\Delta x}\left[R_{w_2\dot{w}_2}(0) + R_{w_2\dot{w}_1}(0) - R_{w_1\dot{w}_2}(0) + R_{w_1\dot{w}_1}(0)\right] \qquad 2.11$$

For a simple sine-wave propagating in the x-direction , the power transmission in the same direction will turn out to be

$$\langle P \rangle_t = \frac{1}{2}TA^2k\omega = 2A^2\pi^2f^2mc \qquad 2.12$$

2.3 Vibration intensity in a beam or a plate

Propagating waves in thin beams or plates can be classified into three major groups: longitudinal waves, transverse waves, and flexural waves. But for the investigation of structure borne noise, the most important propagation mechanism to consider is flexural wave motion, since its resulting lateral displacements create significant pressure waves in the surrounding medium. The beam is assumed to adhere to the assumptions which define the Bernouli-Euler theory.

Consider a beam subjected to flexural wave motion as in Fig.2.1.

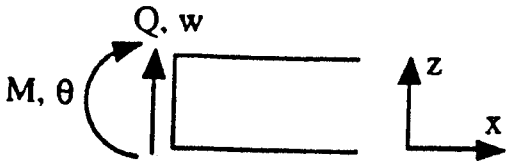

Fig. 2.1. Forces acting on a beam subjected to flexural wave motion

The governing partial differential equation for the transverse displacement of the flexural waves can be obtained in the form

$$D\frac{\partial^4 w}{\partial x^4}+m\frac{\partial^2 w}{\partial t^2}=0 \qquad 2.13$$

and its general solution is of the form

$$w(x,t)=(C_1e^{ikx}+C_2e^{-ikx}+C_3e^{kx}+C_4e^{-kx})e^{iwt} \qquad 2.14$$

where the first two terms include far-field effects and the last two terms include near-field effects and the term k is defined as

$$k^4=\frac{m\omega^2}{D} \qquad 2.15$$

The time averaged intensity or power flow per unit length is given by the equation

$$\langle P\rangle_t=\left\langle Q\frac{\partial w}{\partial t}+M\frac{\partial \theta}{\partial t}\right\rangle_t=D\left\langle\frac{\partial^3 w}{\partial x^3}\frac{\partial w}{\partial t}-\frac{\partial^2 w}{\partial x^2}\frac{\partial^2 w}{\partial x\partial t}\right\rangle_t \qquad 2.16$$

If the near-field effect can be neglected, it can be easily shown that the bending moment term and shear force term are the same, so that,

$$\langle P \rangle_t = 2D\left\langle \frac{\partial^3 w}{\partial x^3}\frac{\partial w}{\partial t}\right\rangle_t = -2D\left\langle \frac{\partial^2 w}{\partial x^2}\frac{\partial^2 w}{\partial x \partial t}\right\rangle_t \qquad 2.17$$

Since, the second partial derivative of the far field solution is $-k^2 w(x,t)$, the above solution can be simplified to be

$$\langle P \rangle_t = -2Dk^2\left\langle \frac{\partial w}{\partial x}\frac{\partial w}{\partial t}\right\rangle_t \qquad 2.18$$

Applying finite-difference approximations we get

$$\langle P \rangle_t = -2Dk^2\left\langle \frac{(w_2 - w_1)}{\Delta x}\frac{(\dot{w}_1 + \dot{w}_2}{2}\right\rangle_t \qquad 2.19$$

Taking cross-correlation to the above terms this equation can be modified as

$$\langle P \rangle_t = -\frac{Dk^2}{\Delta x}\left[R_{w_2\dot{w}_1}(0) + R_{w_2\dot{w}_2}(0) - R_{w_1\dot{w}_1}(0) - R_{w_1\dot{w}_2}(0)\right] \qquad 2.20$$

These cross-correlation terms can be transformed in to the frequency domain by using he following Fourier transform,

$$S_{ab}(x,\omega) = \frac{1}{2\pi}\int_{-\infty}^{\infty} R_{ab}(x,\tau)e^{-i\omega\tau}d\tau \qquad 2.21$$

If we consider the Fourier transform of Eqn. 2.18, the intensity spectrum is

$$\Pi(\omega) = 2\,\mathrm{Re}\left[-Dk^2 \frac{\partial W}{\partial x}\dot{W}^*\right]$$

$$= \frac{Dk^2}{\omega\Delta x}\mathrm{Im}\left[(\dot{W}_1 - \dot{W}_2)(\dot{W}_1^* + \dot{W}_2^*)\right]$$

$$= \frac{Dk^2}{\omega\Delta x}\mathrm{Im}\left[S_{11} + S_{12} - S_{21} - S_{22}\right]$$

which is simplified to

$$\Pi(\omega) = \frac{2\sqrt{mD}}{\Delta x}\mathrm{Im}\left[S_{12}\right] \qquad 2.22$$

For a sinusoidal wave propagating in the x-direction, the power flow will turn out to be

$$\langle P \rangle_t = Dk^3\omega A^2 \qquad 2.23$$

We use velocity terms in deriving equations for power flow because the laser-doppler sensors measure surface velocity. Displacement terms can be obtained by integrating the velocity signals.

CHAPTER 3

EXPERIMENTAL SETUP

3.1 Infinite loop machine - setup

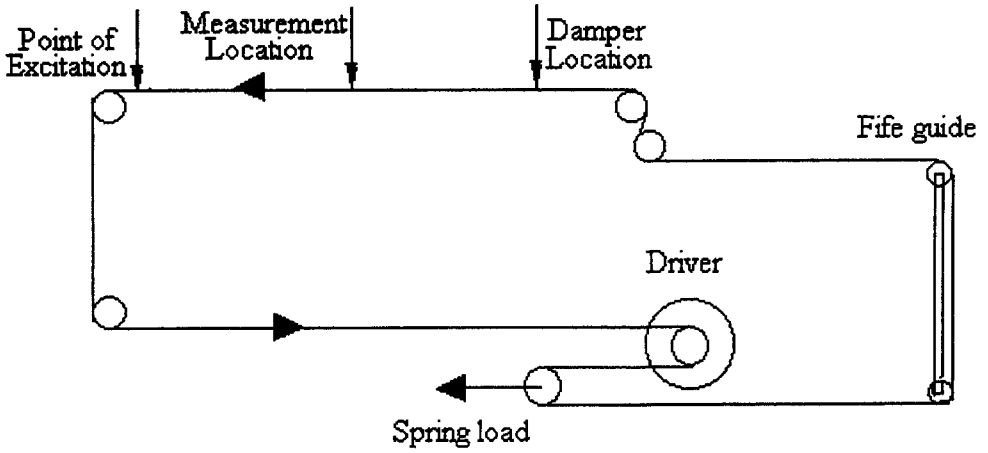

Fig. 3.1. Infinite loop machine (front view of the test setup)

The 2-point intensity measurement technique for a simple web, basically a membrane, was verified in an infinite loop machine, which was equipped with a Fife guide for adjusting the lateral instability of the web. The front view of the infinite loop machine is illustrated in Fig. 3.1. A paper tape was wound around the driver roller to prevent the web slippage on the driver roller. The upper bound of the machine speed is 1300 ft/min. An upwind edge protector was installed to the wind tunnel in order to prevent the vertical deflection of the upwind edge.

In the earlier work done by Cho [2], the vibration characteristics of the machine were examined at 290 ft/min, 620 ft/min and 960 ft/min and the frequency components observed were 9.5 Hz, 18.8 Hz, and 28.3 Hz respectively. These frequencies are well below the operating frequency ranges for the present experiments. All the experiments were conducted with a stationary web. The material of the web used was Polystyrene of 2.6 mil thickness; the mass density of the web was 3.92 e -5 lbm/sq.in.

The web was subjected to tension by the use of spring loads. The tension in the web can be varied by increasing or decreasing the spring load. The spring system has a set of two springs mounted parallel to each other and a lead screw provides the linear motion for the springs.

3.2 Instrumentation for Excitation of web

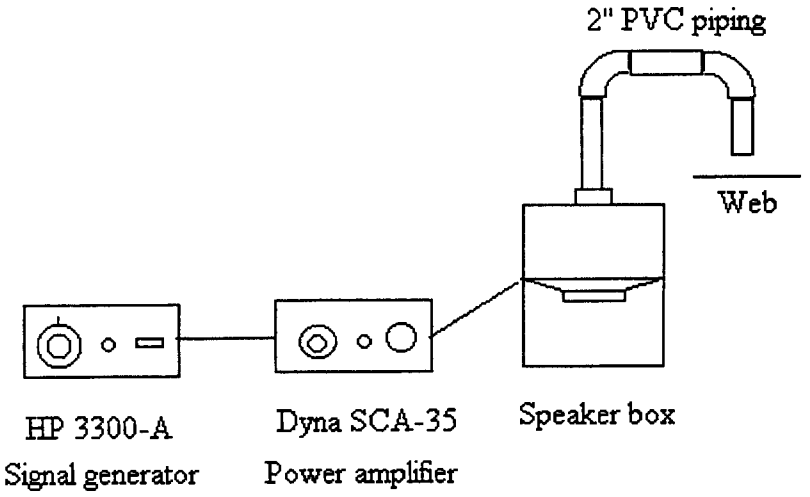

Fig. 3.2. Instrumentation for excitation of the web

The web was excited at different frequencies and the instrumentation for this is illustrated in Fig. 3.2. A two channel HP 3300-A function generator with an 3301-A

auxiliary plug-in was used to generate signals of known frequency and amplitude. This signal generator is capable generating triangular, square, and sine waves and the frequency ranges of the generated signals are 0.01 Hz to 100 KHz. This signal being not strong enough to excite the speaker, a Dyna stereo SCA-35 amplifier was used to boost the signal. This amplifier was equipped with a tape head, phono, radio, tape, and spare. It operates at 50 to 60 Hz. AC cycles and has a 600 W max. AC outlet. The signal from the amplifier was then fed to the speaker which was mounted in a rectangular box facing the cone upwards. This box was made of fiber wood and has flange openings on both ends.

A 2" PVC piping was used to transfer the excitations from the speaker to the web. The open end of the piping was placed right above the web near a roller support. The air inside the speaker box is excited by the signal generator, which flows through the piping and in turn excites the web. The natural frequency of excitation of the piping system was found to be 8.5 Hz which is far below the experimental frequency ranges.

3.3 Data Acquisition - Instrumentation

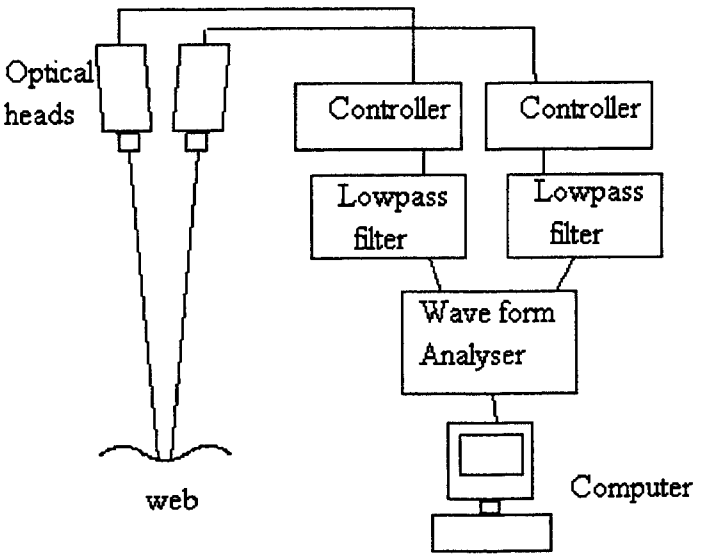

Fig. 3.3. Instrumentation for data acquisition

According to Mitjavila[11], the use of piezo-electric transducers will have a significant effect because of their added mass to the structure . Hence, strain gauges and laser techniques are suggested in cases where the mass of the structure under consideration is fairly small. A two laser vibrometer setup was used to measure the wave properties, such as frequency, amplitude, phase and wave speed, of the vibration in the web along the flow direction as shown in Fig. 3.3.

For the case of normal incidence of the laser beams, the reflected beams were too strong to measure the vibration of the web. To avoid this problem and to adjust the distance between the measuring points, the vibrometers were tilted slightly. The distance between the two measuring points was 7.5 mm. The operation ranges of the laser vibrometers are 1 E -10 m to ~ 1 m in displacement, 5 E -10 m/s to ~2 m/s in velocity and 1 E -6 m/s^2 to ~ 1 E 5 m/s^2 in acceleration. The controllers have the capability of adjusting the resolution of the measured signal.

It was observed that the reflecting signal was weak therefore, a small thin tape(5 mm X 15 mm) of reflecting material was placed on the web where the measurement takes place. The dominant frequencies of experimentation were below 300 Hz. Therefore, the signal from each laser vibrometer was filtered by a low-pass filter with a cut-off frequency of 600 Hz. The maximum number of sampling points of the wave form analyzer were 8192, the range of the sampling period was 60 μ sec. to ~ 600 sec. and the resolution of the magnitude was 14 bits.

For the case of calculating the intensity, apart from phase angles and amplitudes at certain frequencies, a complete history of the velocity of the two measuring points is necessary. The HP spectrum analyzer equipped with a disk drive uses a HP instrument LIF (Logical Interchange Format) and can save the velocity signal traces in a SDF (Standard Disk Format). Though the wave form analyzer has the facility of frequency domain analysis, the data were saved in the time domain to facilitate the determination of

dominant frequency components and calculation of phase angles and phase differences. The wave form analyzer has a sampling time ranging from 7μ Sec to 60Sec. The sampling frequency was set at 1 Hz and the number of points for each set of data being 512.

3.4 Experimentation

3.4.1. Calibration of the spring mounting.

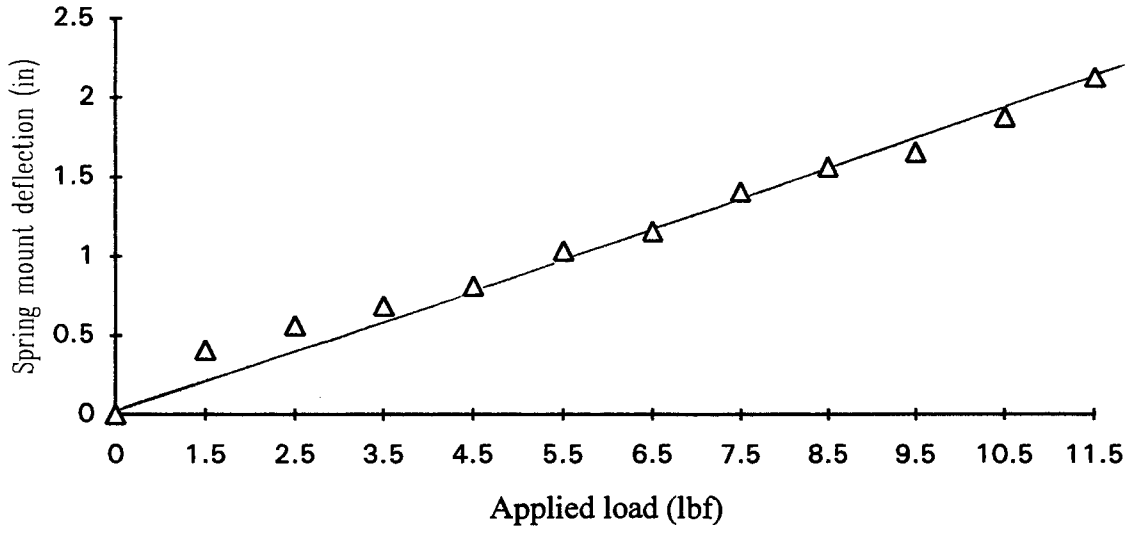

Fig. 3.4. Calibration of the spring assembly

In order to determine the tension in the web the spring constant of the assembly has to be determined. Instead of calibrating the springs separately, and calculating the spring constant of the assembly, the springs were calibrated as an assembly by cutting open the infinite loop, fixing one end of the web to the Fife guide roller and applying loads at the other end. The characteristic of the spring assembly is as shown in Fig. 3.4. The practical limit of the tension in the web through the spring load was found to be

11.48 lbf. but for the experimentation very low values of tension were used, as can be explained later. The two values of tension used in the experiments are 1.48 lbf and 2.48 lbf.

3.4.2. Phase difference calibration of the instruments

Since the intensity measurement technique is very sensitive to phase-errors, the measuring instruments have to be calibrated. Phase-mismatch between the two laser sensors, and phase errors between the two low pass filters are the possible errors that can be introduced due to the instruments. To check the phase mismatch between the sensors, both the sensors were focused on the central part of a speaker cone and the phase angles are measured. Since, the central part of a speaker cone behaves like a piston, theoretically the phase difference between the speakers is supposed to be zero. The values obtained in the experiment indicate that there is no phase mismatch between the sensors.

The phase error can also be introduced due to the low pass filters. The signal from the signal generator is fed to the filters and the phase difference between the two filters is measured. The measurements show that there is significant phase-difference between the filters. The phase difference characteristic of the filters is shown in Fig. 3.5.

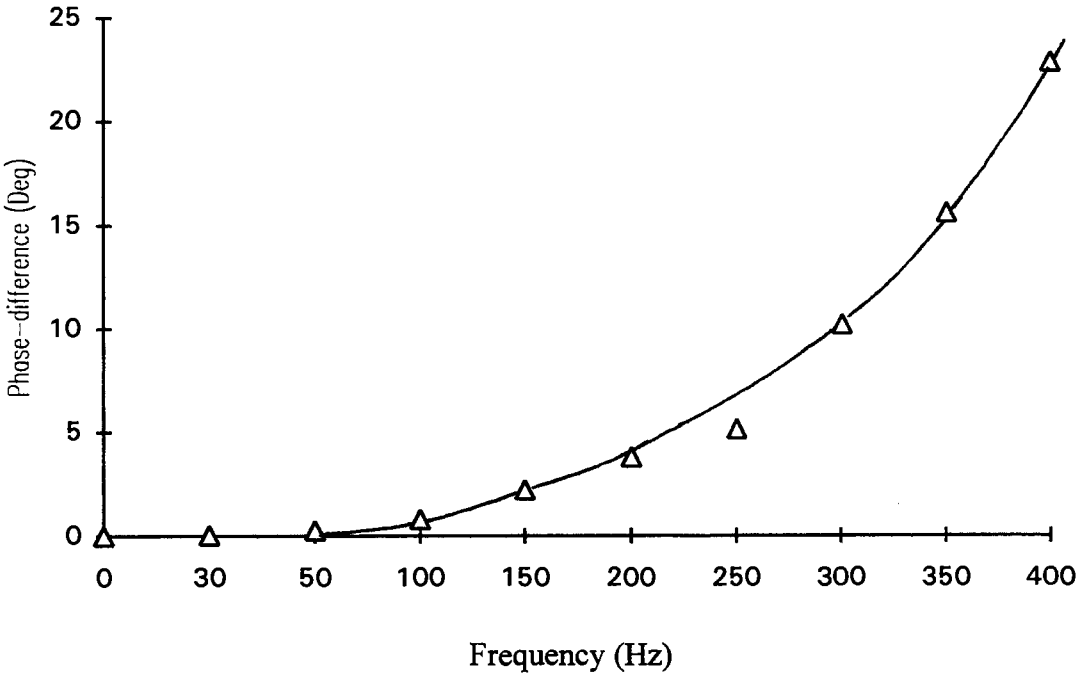

Fig. 3.5. Phase difference characteristic of the low pass filters

3.4.2. Development of wave patterns.

Standing and traveling waves are developed in the web by modifying the boundary conditions. To obtain a standing wave, roller supports are placed at both extremes of the web span. The support at the excited end is given by a simple roller support, and the support at the far end is given by passing the web between two rollers.

To develop a traveling wave, several boundary conditions were tested. Experiments were conducted by making slots in the web to facilitate dissipation of the wave energy. But, this alters the tension distribution in the web and also, the web becomes weak at this point. Damping materials were placed at the ends to absorb the wave energy, and reduce the reflected wave. Since any sudden change of impedance causes reflections, a wedge shaped damper was used. The angle of the wedge was also

reduced to improve the effect. Different configurations tried are shown in Fig. 3.6. and the configuration in Fig. 3.6.f was found to be the best of all.

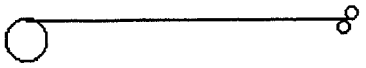

Fig.3.6.a Roller support at both ends

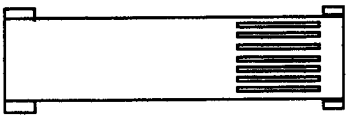

Fig.3.6.b. Web with slots at the far end (Top view)

Fig.3.6.c. Wedge shaped damper at both ends

Fig.3.6.d. Damping at far end on both sides

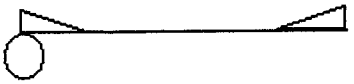

Fig.3.6.e. Damper with smaller wedge angle

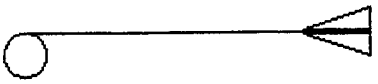

Fig.3.6.f. Damper at far end on both sides(small wedge angle)

Fig. 3.6. Different configurations used to develop wave patterns

3.4.3. Calculation of the wavelength.

The assumptions made, regarding the free-field measurement, necessitate the calculation of the wavelength theoretically and to compare it with the experimentally measured value. Also, these assumptions impose certain bounds for the wavelength to make the intensity measurements valid. One of the assumptions is that the web behaves in a string mode, such that the wave speed and other wave properties can be calculated.

The wave speed for a string is given by

$$c = \sqrt{\frac{T}{m_w}} \qquad 3.1.$$

and the wave length is given by

$$\lambda = \frac{c}{f_{ex}} \qquad 3.2.$$

But, in the above case, the radiation impedance of unbaffled web (a web having free edges only) is not considered. The interaction of the web and stationary air has to be considered as a circular piston. The radius of the piston is given by

$$r = \sqrt{\frac{Ld}{\pi}} \qquad 3.3$$

where L and d are length of the web in machine direction and width of the web in cross-machine direction respectively. The mass of this circular piston of air according to Chang [1], is given by

$$m_a = c_a \frac{\pi}{4} \rho d \qquad 3.4.$$

where $\phi = 2\pi \frac{\Delta\tau}{\Delta T}$, the added mass coefficient, is 1.0. in cases where the slenderness ratio L/d is very large, or if the web is slender.

the radiation impedance for ripples having a short wavelength can be calculated as follows. Consider a traveling wave in a web as in the case under consideration, where $\lambda << d$ and $\lambda << L$. The added mass of air can be calculated as

$$m_a = \frac{\rho\lambda}{\pi} \qquad 3.5$$

The wave speed can now be calculated as

$$c = \sqrt{\frac{T}{m_w + m_a}} \qquad 3.6.$$

Since the calculation of the air mass involves the wave length, which in turn depends on the wave speed, a numerical iteration process has to carried out to determine the wave length of the traveling wave in the web.

Sample Calculation:

Test Conditions

$T = 0.185$ lbf/in.

$m_w = 3.92$ e -5 lb/sq.in.

$\rho = 4.674$ e -5 lb/ cu.in.

$f_{ex} = 400$ Hz.

Neglecting the mass of air, the wave speed c = 1350.6 in/sec.

and the wave length λ =3.375 in.

the mass of air can be calculated from Eqn. 3.5. and m_a = 5.022 e -5 lb/sq.in.

now the wave speed can be calculated from Eqn 3.6 and c= 894.1 in/sec.

From this, the wave length is calculated and again the mass of air, and these iterations are repeated to get the exact value of wave length, a wave speed and mass of air. After a few successful iterations the values obtained are

c= 894.1 in/sec.

λ =3.375 in.

and m_a = 5.022 e -5 lb/sq.in.

These calculations are repeated for different test conditions to obtain the exact wave characteristics.

3.4.4. Calculation of Phase Differences.

It is evident that the intensity or power flux flowing across a web is zero for a standing wave. So, it is essential to have a traveling wave in the web to make the intensity measurements meaningful. To determine whether the wave under consideration is traveling wave or not, the phase difference between the two measuring points is a key characteristic. For particular set of test conditions, the theoretical wave length and wave speed are calculated as shown above.

The phase difference between two measuring points in a wave is given by

$$\phi = \frac{\Delta x}{\lambda}.2\pi \qquad 3.7.$$

where Δx is the spacing between the measuring points.

The experimentally measured values of the phase differences are compared with these theoretically calculated values. Phase differences can be experimentally measured either by spectral methods or correlation methods. In the spectral method the time domain signals of the two measuring points are transformed to frequency domain by applying Fourier transforms, and the phase difference of the two signals is found at the dominant frequency, which in this case is the excitation frequency. The phase difference by this method is calculated as

$$\phi = \phi_2 - \phi_1 \qquad 3.8.$$

The correlation method gives the phase differences between the two spectra in time domain. The cross-correlation of two signals is given by Eqn 2.10. and, the phase difference between two signals can be determined by

$$\phi = 2\pi \frac{\Delta\tau}{\Delta T} \qquad 3.9.$$

For the case of the experimentation , the spectral method was chosen since it gives the phase differences directly at the dominant frequencies and is not sensitive to the sampling frequency.

3.5 Test Procedure

Experiments were conducted on a particular web material with two different tensions and different excitation frequencies. The testing was done with the following procedure.

1) The location of the measuring points was set and the distance between the measuring points was adjusted by slightly adjusting the angle of the laser beams.

2) The web tension was set to the required value by adjusting the lead screw which gives feed to the spring mounting.

3) The web was fixed at its extreme ends over the rollers by an adhesive tape.

4) The pattern of the wave was set to either traveling to standing by placing a wedge shaped damper or a roller support respectively.

5) The signal generator was set to the required excitation frequency.

6) The amplitude of the signal was adjusted so that a clear signal can be observed in the wave form analyzer.

7) The wave characteristics such as frequency, phase difference at different test conditions are measured save the data saved in a HP wave form analyzer for further calculations.

8) The data are converted from SDF to DOS using certain algorithms supplied with the instrument and calculation algorithms are used to compute the intensity.

CHAPTER 4

RESULTS AND DISCUSSIONS

This chapter presents and discusses the results obtained in the experiments. The measurements were made in the far field of the web under consideration. The near field effects can be eliminated by taking measurements away from the discontinuities and boundaries and disturbing sources. Also, the web is assumed to behave like a string (or a one-dimensional membrane). To make these assumptions valid, it is necessary to customize the experimental parameters and the procedure. Since the power flow in a standing wave is theoretically zero, a traveling wave has to be considered for the case of measurement and analysis.

To validate the assumptions made above, a mathematical model has to be considered and the results obtained have to be compared with experimentally measured values. The phase angles wave lengths and wave speed have to be calculated from theory and compared with the measured values. To establish the fact that there is a traveling wave there has to be a fixed amount of phase difference between the two measuring points, as can be calculated from the theory explained in earlier chapter.

To support the assumptions made regarding far-field measurement,

1) The measurement should be taken at least two to three wave lengths away from any discontinuities, boundaries or disturbing sources.

2) The distance between the measuring points should be a fraction of the wave length (less than quarter of the wave length).

3) The distance between measuring points affects the finite difference error. so it has to be small (in the working range of 8-10 mm).

4.1. Discussion of low frequency measurements

Initially, experiments were conducted using the wind tunnel as a source of excitation, and the measurements indicated a major frequency component of 23.4 Hz. Measurements at this frequency range failed to give a good estimate of wave characteristics, due to the fact that measuring points are very close to the boundary, and due to resonance caused by the natural frequencies of the system. In order to avoid these problems, the web was excited by an acoustical system.

The natural frequency of the PVC piping system was 8.5 Hz, and those of the setup were 10 HZ, 19 Hz, and 28 Hz. These frequencies have significant higher harmonic components also. Experiments were conducted on a web with a tension of 0.185 lbf/in.by externally exciting the web at 5Hz, 10 Hz, 20 Hz, 30 Hz, 50 Hz, and 60 Hz. The wave lengths of these measurements are plotted in Fig.4.1. As can be seen, the values are away from theoretical curve. Also, the data were found to be inconsistant. The reasons for this can be the resonance due to the natural frequencies of the system. Also, to make the assumptions regarding the far-field valid, the frequencies for the measurements chosen are above 100 Hz, where the resonance effect can also be neglected.

4.2. Comparison of Wave lengths

The decision was made to narrow the range of the wavelength to 2-7 inches. The wave length calculation was performed for different tensions in the web at different excitation frequencies and these values are compared with those obtained from experiment. Fig. 4.2. shows the wavelength values obtained for a tension value of 0.185 lbf/in. and Fig. 4.3. shows the comparison for a tension value of 0.31 lbf/in. For a particular tension, increasing the excitation frequency results in a lower value of wave length. At a given excitation frequency an increase in tension directly results in a higher

value of the wave length. These trends are seen in the experimental values only at certain frequencies.

The deviation from the theoretical curve at low frequencies can partly be explained by the resonance caused due to these natural frequencies of the system. The experimental values are in close agreement with theory at excitation frequencies of 150 Hz, 200 Hz, and 250 Hz, since these are well above the natural frequencies of the system. An increase in tension results in an increase in wave length, and to bound the wave length in the range to validate the free-field assumptions, higher excitation frequencies have to be chosen. Measurements at high excitation frequencies (around 400 Hz) and high value of tensions (around 0.56) were performed and the displacement amplitudes were found to be very small. Based on these observations, tension values of 0.185 lbf/in. and 0.31 lbf/in, and excitation frequencies of 150 Hz, 200 Hz, and 250 Hz are chosen for the study of intensity calculation.

4.3. Comparison of Phase Differences.

Phase difference between the measuring points is a good tool to determine whether the wave under consideration is a standing wave or traveling wave. A standing wave pattern is established in the web by placing the web between two fixed supports. Table.4.1. shows the phase differences for a stationary wave from experiments. Theoretically these values are supposed to be zero. Though the measured phase differences are not exactly zero, these small values can be neglected, since there is a phase error introduced by the filters, and the wave can be considered as a standing wave. Though these values are not of use in intensity calculations, they are consistent with the theory.

Intensity measurements carry a sense only when the measurements are done on a traveling wave. It is essential to establish that there is a traveling wave, and this can be

achieved by comparing the computed phase differences with the measured values. Table.4.2 shows the phase differences for a traveling wave, both measured and computed. These values obtained from the experiments are in good agreement with the theory. At lower tension values, the phase angles are relatively high. For a particular tension value, an increase in the excitation frequency results in a higher value of phase difference. At a given excitation frequency, an increase in tension yields a lower value of phase difference. These trends can be observed in the experimental data of phase angles.

Since, for a traveling wave, the amplitude at any point on the wave is constant, the amplitudes at the two measuring points can be compared. Table 4.3. shows the amplitudes of vibration velocity at the two measuring points. These values are very close to each other and confirm that the wave under study is a traveling wave.

Also, the wave patterns were observed by use of a stroboscope to check for any nodal points. Any major component of standing wave results in nodal points, which can be observed using a stroboscope, and in the observations no nodal points were seen. This observation also, confirms the traveling wave.

4.4. Comparison of Intensity or Power flux.

Now that the basic assumptions made have been validated, we can consider computing the intensity or power flow that is being transmitted along the machine direction of the web. The intensity measurements were done at the same test conditions. The finite-difference error for the intensity calculation algorithms was found to be 2.3 % and this is considered small enough to be neglected.

The intensity per unit width for 0.185 lbf/in tension at different excitation frequencies has been illustrated in Fig.4.4. The intensity value drops with an increase in excitation frequency. This is an indicative of the decrease in the flutter velocities. A plot for a tension value of 0.31 lbf/in. at three excitation frequencies is illustrated in Fig. 4.5.

It can be seen that the amount energy flow drops with an increase in excitation frequency. It can, also, be observed that the drop in the intensity is not considerable with an increase in excitation frequency from 200 to 250 Hz. This can be explained from the calculations for the wave length. The wave length reaches a value and the decrease in wavelength is not proportional to the increase in excitation frequency in this region.

Fig.4.6 shows the power flow at two tensions0.185 lbf/in and 0.31 lbf/in., at an excitation frequency of 150 Hz. The minor shift in the peaks of the intensities is because the signal generator is an analog function generator and the generated frequency is a little smaller or larger than the set value. This figure gives an idea of how the tension effects the intensity flow. The higher values are obtained for higher values of tension. So, the techniques involving inducing tension to suppress the web flutter actually cause more amount of power to flow across the web. A similar plot is illustrated in Fig. 4.7. at an excitation frequency of 200 Hz. From these two graphs the amplification factor with an increase in tension at different excitation frequencies was found to be approximately 4 and 2.72 at excitation frequencies of 150 and 200 respectively. This drop in this factor indicates the reduced effect of tension at higher frequencies.

Intensity flowing across the structure, a web in this case, as observed from the experimental values, gives an impression of how much energy is flowing, in what direction and at what dominant frequencies. If a proper correlation can be developed between the theoretically predicted values and observed values, it will be of significance. In real cases, there will not be a perfect traveling wave or a pure standing wave, but a mixture of both. The intensity of a standing wave being zero, the intensity flow in a mixed case will be difficult to predict. A comparison of theoretical and experimental values of intensity has been presented in Table 4.4. The intensity flow across a string is given by Eqn.2.11. and for a pure sinusoidal wave the intensity is given by Eqn. 2.12.

The minor discrepancies in this table can be explained, in part, that the string mode behavior of the web may not be completely valid. The bending stiffness of the web

contributes in part to the total power flow and this is being neglected. These predictions give us a trend that at higher flutter amplitudes the power flow is high, and as the flutter amplitude decreases the power flow also decreases. This trend can be observed in both experimental and theoretical values.

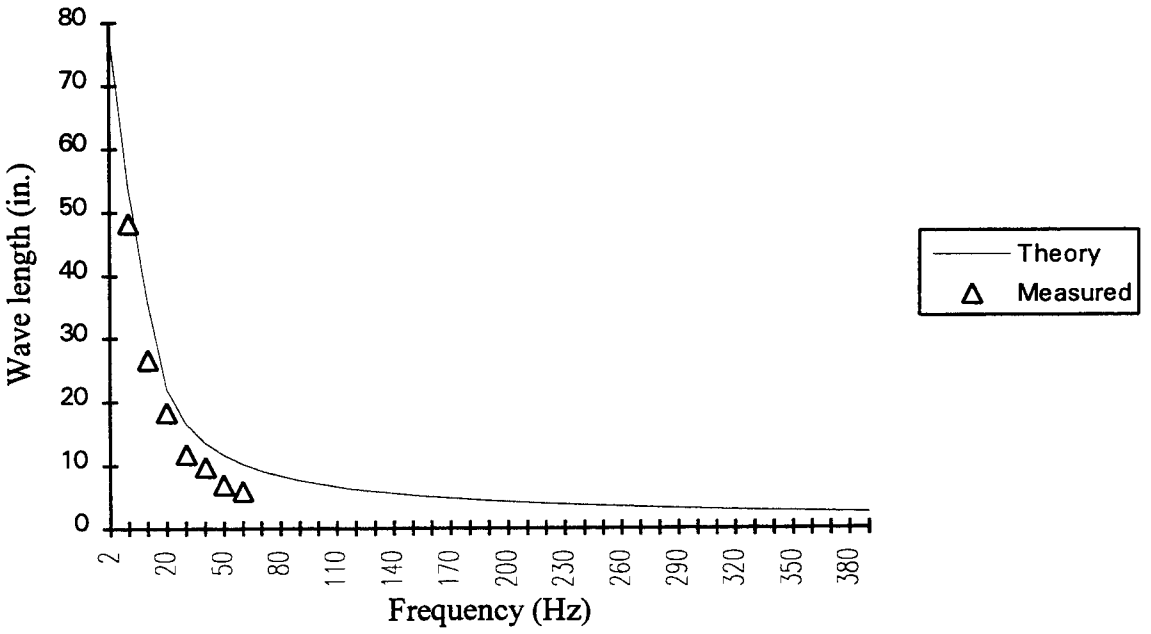

Fig. 4.1. Wave length data for low frequency measurements

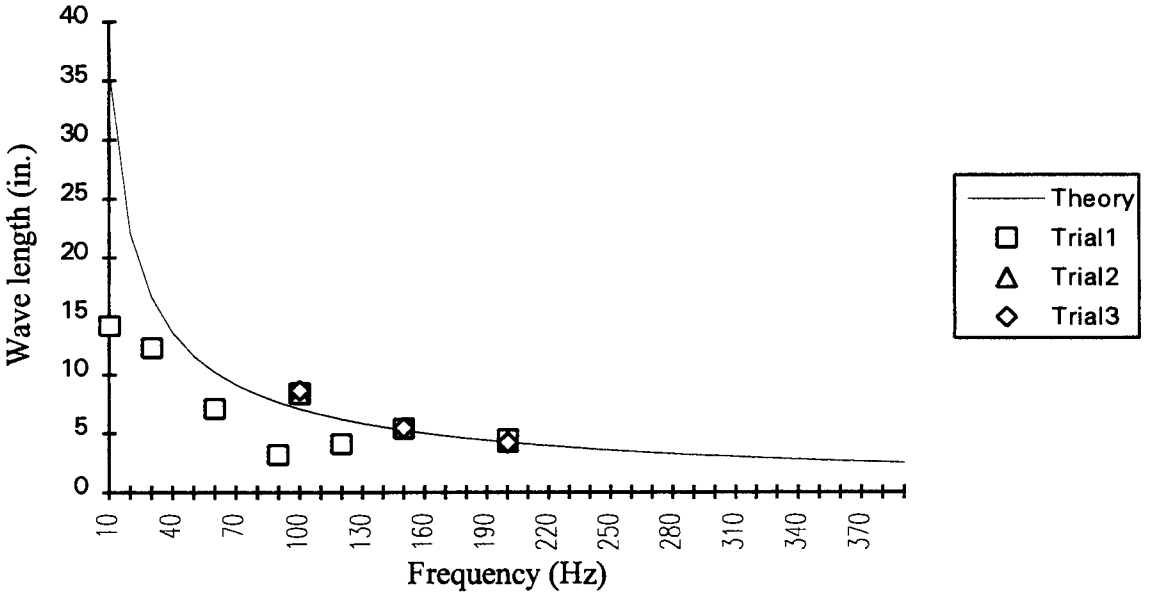

Fig.4.2. Comparison of wave lengths at 0.185 lbf/in. tension.

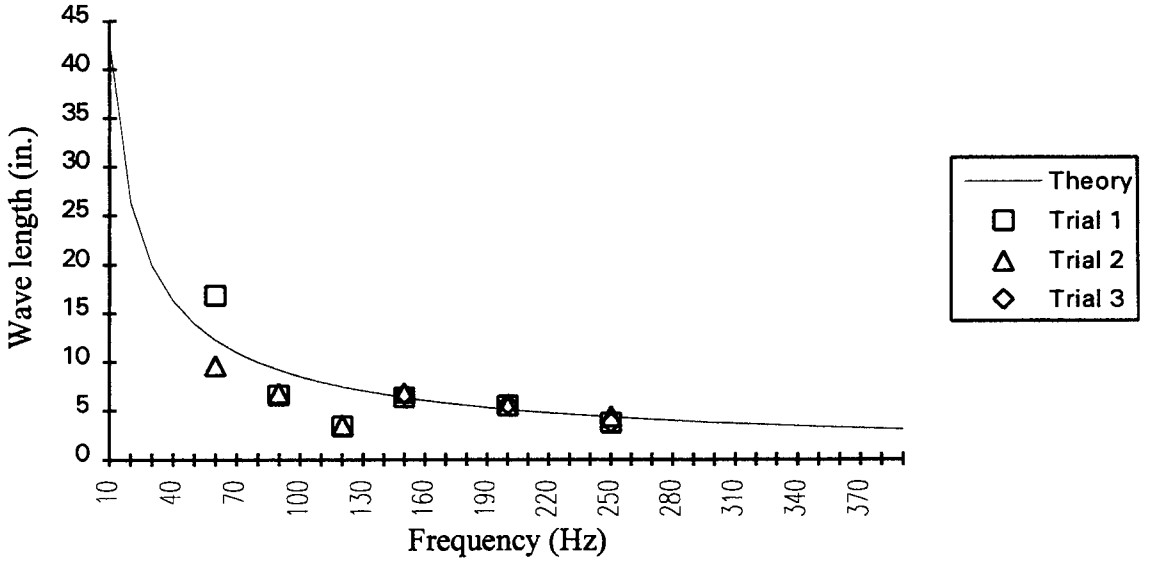

Fig.4.3. Comparison of wave lengths at 0.31 lbf/in. tension.

Tension (Lbf/in.)	Excitation Frequency (Hz.)	Phase Difference Measured (Deg.)
0.185	150	3.2
0.185	200	0.59
0.31	150	2.4
0.31	200	2.5
0.31	250	1.6

Table 4.1. Measured phase difference for a standing wave.

Tension (Lbf/in.)	Excitation Frequency (Hz.)	Phase Difference Measured (Deg.)	Phase Difference Theory (Deg.)
0.185	150	23.3	24.5
0.185	200	26.8	30.4
0.31	150	19.6	20.2
0.31	200	23.4	25.0
0.31	250	34.0	29.6

Table 4.2. Measured phase differences for a traveling wave.

Tension (lbf/in)	Excitation Freq.(Hz).	Amplitude of Velocity of point 1 (in/sec)	Amplitude of Velocity of point 2 (in/sec)
0.185	150	0.3145	0.3157
0.185	200	0.3358	0.3245
0.31	150	0.5101	0.5124
0.31	200	0.3840	0.3758
0.31	250	0.2895	0.2883

Table. 4.3. Table showing the peak amplitudes of measuring points 1 and 2

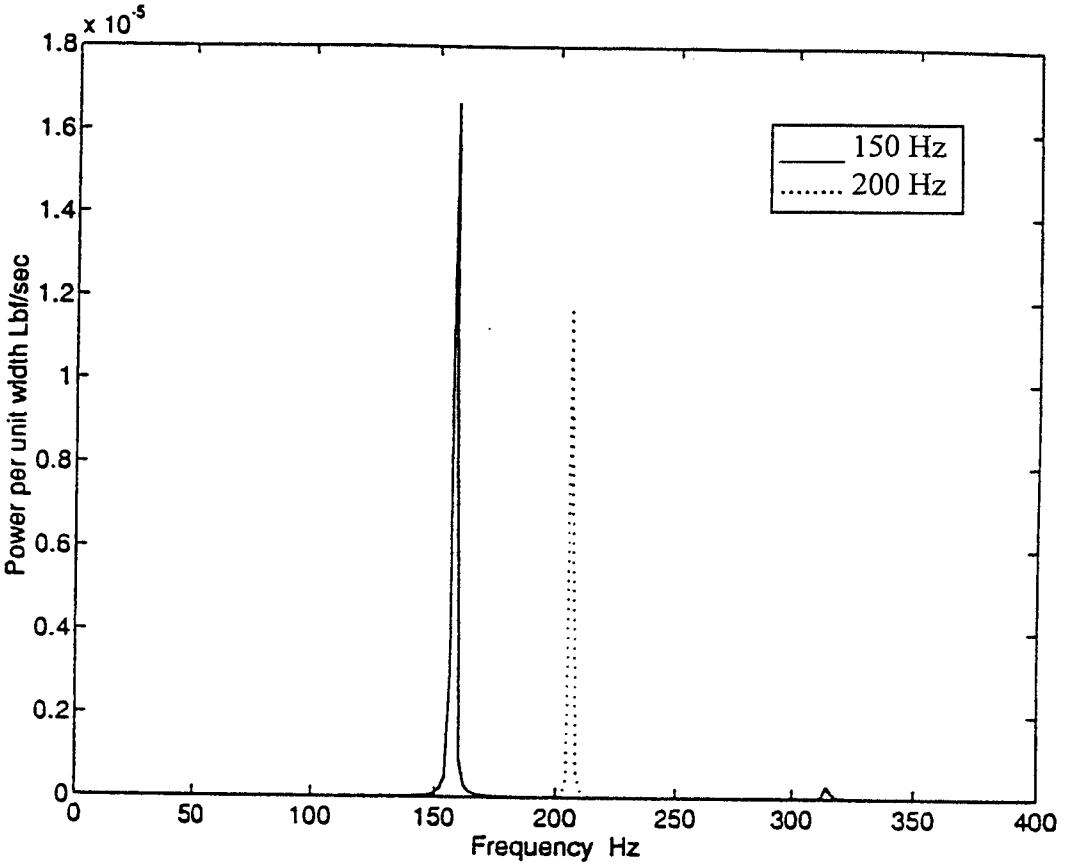

Fig. 4.4 Comparison of power flow spectra for two excitation frequencies at 0.184 lb/in. tension

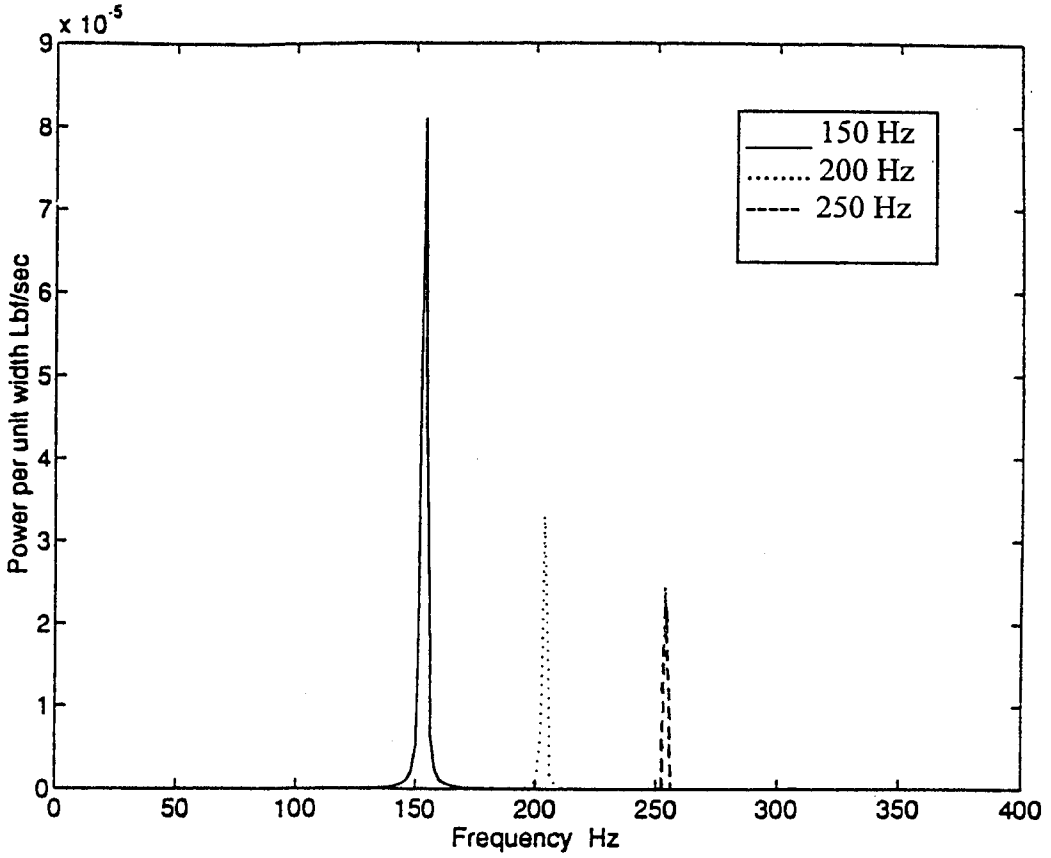

Fig. 4.5 Comparison of power flow spectra for three excitation frequencies at 0.31 lb/in. tension

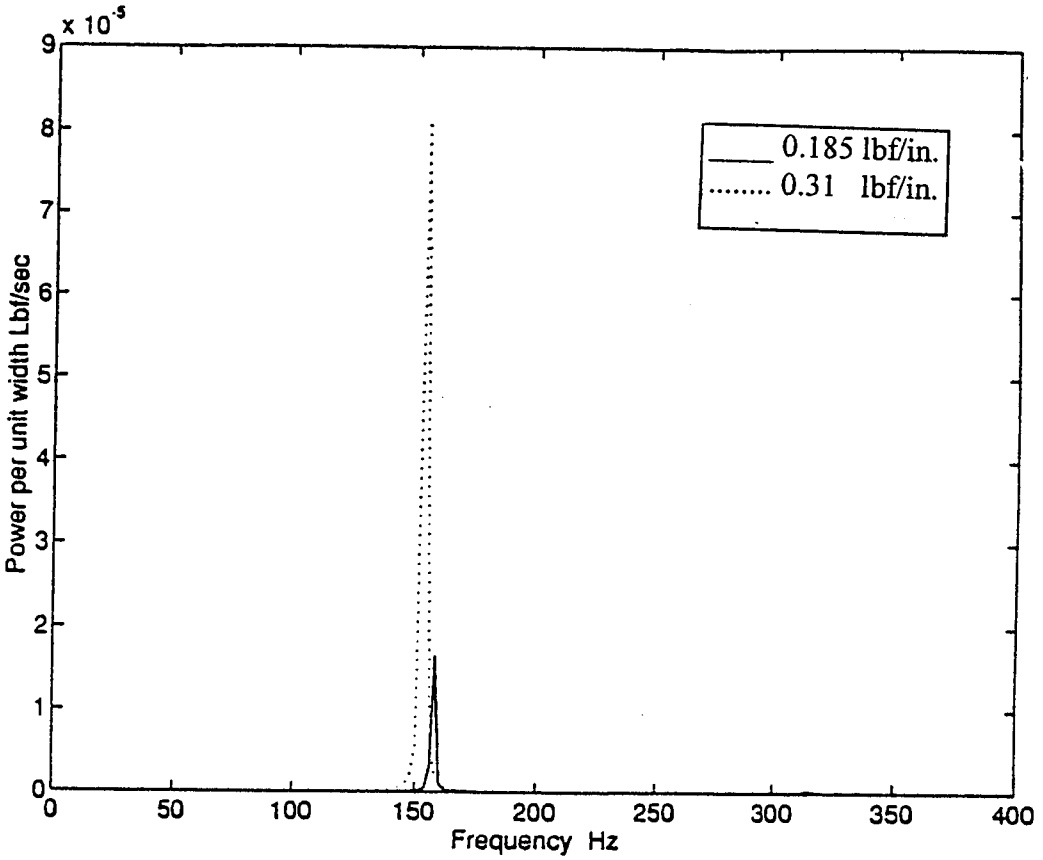

Fig. 4.6 Power flow at two different tensions for an excitation frequency of 150 Hz

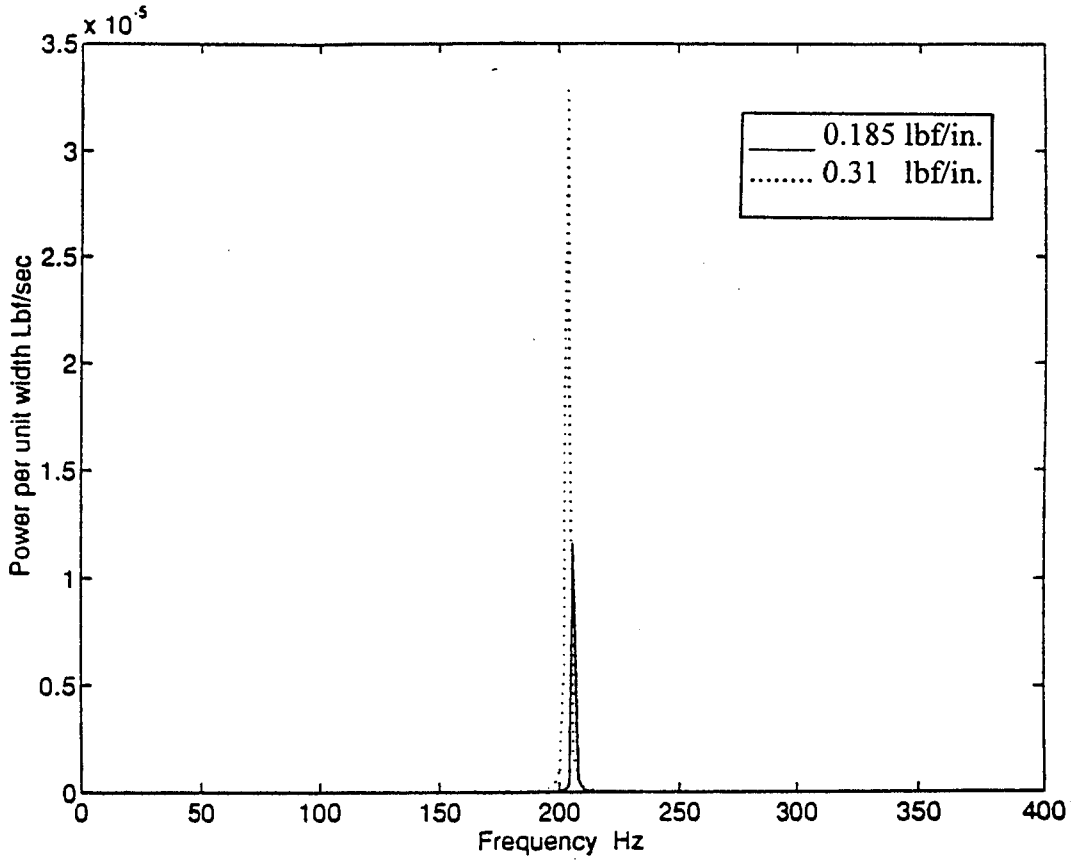

Fig. 4.7 Power flow at two different tensions for an excitation frequency of 200 Hz

Tension (Lbf/in.)	Excitation Frequency (Hz)	Displacement Amplitude in.	Power flow from Theory (Lbf/sec).	Power Flow measured (Lbf /Sec)
0.185	150	3.906 e -4	1.628 e -5	1.68 e -5
0.185	200	2.72 e -4	1.304 e -5	1.18 e -5
0.31	150	7.53 e -4	7.21 e -5	8.1 e -5
0.31	200	3.84 e -4	3.44 e -5	3.3 e -5
0.31	250	2.25 e -4	1.801 e -5	2.4 e -5

Table. 4.4. Comparison of the theoretical and measured power flow values.

CHAPTER 5

CONCLUSIONS AND RECOMMENDATIONS

5.1. Conclusions

From the study in which two Laser Doppler sensors were used to measure the basic wave properties in a web the following conclusions were made:

1.) Wave properties (out-of-plane velocity, frequency, wavelength, phase-difference, and propagation speed) can be measured by use of two laser vibrometers and FFT algorithms.

2.) The magnitude of power flow along the web in the machine direction can be measured by the two laser vibrometer method and an intensity algorithm.

3.) The characteristics of the power flux, such as direction, dominant frequency, phase information etc., can also be obtained from the measurements using intensity algorithms.

4.) Either traveling waves or stationary waves can be established in the web, depending on the boundary conditions.

5.) The effect of air mass is considerable.

5.2. Recommendations for further research.

Though a good agreement has been observed between the measured and analytical solutions this method makes certain assumptions that may not be valid in practical situations. Throughout this study the parameters of the experiments are chosen in such a way as to validate the assumptions made. For a more complex problem, like a wind tunnel excitation, additional measurements have to be made to consider the effect of stiffness, shear, and torsion terms. The following suggestions are made for further research:

1.) To test the intensity technique in the presence of noise and standing waves.

2.) To include the effect of stiffness and shear and perform a 4-point measurement.

3.) To perform a comparative study of 2-point and 4-point measurement in the near-field and far-field.

4.) To repeat the tests with a moving web.

5.) To use the technique for autonomous air-flow-excited flutter.

REFERENCES

(1.) Chang,Y. B., " An Experimental & Analytical Study of Web Flutter " Ph.D., Dissertation, 1990, Oklahoma State University.

(2.) Cho, C. H., " Experimental Study of Edge Flutter of Travelling Webs ", MS Thesis, 1992, Oklahoma State University.

(3.) Cuscheri, J. M., "Structural Power-Flow Analysis Using a Mobility Approach of an L-Shaped Plate," Journal of Acoustical Society of America, 1990, Vol. 87, No. 3, pp. 1159-1165.

(4.) Cuscheri, J. M., "Experimental Measurement of Structural Intensity on an Aircraft Fuselage," Noise Control Engineering Journal, 1991, Vol. 37, No. 3, pp. 97-107.

(5.) Cuscheri, J. M., "Frequency- Wave number Analysis of Structural Intensity," Second International Congress on Recent Developments in Air- and Structure-Borne Sound and Vibration, March 1992, Auburn University, Vol. 3, pp. 1361-1368.

(6.) Downing, J. M., "Power Flow Measurements in a Beam Utilizing a Five Accelerometer Probe," MS Thesis, George Washington University, 1988.

(7.) Gade, S., "Sound Power Determination from Sound Intensity Measurements," Sound and Vibration, December 1989, pp. 18-22.

(8.) Mann, J. A., III, and Tichy, J., "Acoustic Intensity Analysis: Distinguished Energy Propagation and Wave-Front Propagation," Journal of the Acoustical Society of America, 1991, Vol. 90, No. 1, pp. 20-25.

(9.) McDevitt, T. E., Koopmann, G. H., and Burroughs, C. B., "Two-Channel Laser Vibrometer Techniques for Vibrational Intensity Measurements, Part I: Flexural Intensity," ASME Journal of Vibration and Acoustics, 1993, Vol. 115, No. 4, pp. 436-440.

(10.) McGary, C. M., " Simulated Measurements of Power Flow in Structures Near to Simple Souces and Simple Boundaries ", NASA Technical Memeorandum - 89124, 1988.

(11.) Mitjavila, A., Pauzin, S., and Biron, D., "Measurement of Structural Intensity in Thin Plates Using a Far Field Probe," Second International Congress on Recent Developments in Air- and Structure-Borne Sound and Vibration, March 1992, Auburn University, Vol. 3, pp. 1353-1360.

(12.) Noiseux, D. U., " Measurement of Power Flow in Uniform Beams and Plates," Journal of the Acoustical Society of America, 1970, Vol. 47, No. 1 (Part 2), pp. 238-247.

(13.) Pavic, G., "Measurement of Structure Borne Wave Intensity, Part I: Formulation of Methods," Journal of Sound and Vibration, 1976, Vol. 49, No. 2, pp. 221-230.

(14.) Piaud, J. B., and Nicolas, J., "Relationship Between Vibrational and Acoustical Intensity for an Infinite Plate," Journal of the Acoustical Society of America, 1986, Vol. 80, No. 4, pp. 1114-1121.

(15.) Pierce, A. D., "Physical Interpretation of the WKB or Eikonal Approximation for Waves and Vibrations in Inhomogeneous Beams and Pipes," Journal of the Acoustical Society of America, 1970, Vol. 48, No. 1 (Part 2), pp. 275-284.

(16.) Pope, J., "The Two-microphone Sound Intensity Probe," ASME Journal of Vibration, Acoustics, Stress and Reliability in Design, 1988, Vol. 110, No. 1, pp. 97-103.

(17.) Rasmussen, G., "Intensity - Its measurement and Uses," Sound and Vibration, 1989, March, pp. 28-33

(18.) Rasmussen, G., "Source Location Using Vector Intensity Measurements," Sound and Vibration, 1989, March, pp. 28-33

(19.) Shirahatti, U. S., and Crocker, M. J., "Studies on Sound Power Measurements Using the Sound Intensity Technique," Noise Control Engineering Journal, 1993, Vol. 41, No. 2, pp. 323-330

(20.) Thornton, W. R., "Intensity Measurement - Past, Present and Future," Sound and Vibration, 1989, March, pp. 5.

(21.) Upton, R., "Sound Intensity - A Powerful New Measurement Tool," Sound and Vibration, October 1982, pp. 10-18.

(22.) Verheij, J. W., "Cross Spectral Density Methods for Measuring Structural Borne Power Flow on Beams and Pipes," Journal of Sound and Vibration, 1980, Vol. 70, No. 1, pp. 133-139.

(23.) Verheij, J. W., "Measurements of Structure-Borne Wave Intensity on Lightly Damped Pipes," Noise Control Engineering Journal, 1990, Vol. 35, No. 2, pp. 69-76.

(24.) Williams, E. G., Dardy, H. D., and Fink, R. G., "A Technique for Measurement of Structure-Borne Intensity in Plates," Journal of Acoustical Society of America, 1985, Vol. 78, No. 6, pp. 2061-2068.

APPENDIX A

LIST OF INSTRUMENTS USED

INSTRUMENT	SPECIFICATIONS
Function Generator HP 3300-A	Sine, Square, and triangular waves Freq. range 0.01 Hz - 100 KHz
Power Amplifier DYNA SCA-35	Tape head, Radio, Phono and spare connections 600 W max AC outlet.
Laser Sensors Polytec OFC-350	Helium Neon laser 1 mW Max. power
Controllers Polytec OFC-2600	Vibrometer controls are 125 mm/sV, 25 mm/sV and 5mm/sV
Filters Multimetrics AF-120	2 Channel low pass and high pass 20 HZ to 2 MHz
Signal Analyzer HP 35665 A	2 Channel, DOS and LIF formatted drive.
Signal Analyzer DATA 6100	4 Channel spectrum analyzer, built in programming type.

VITA

Vedula Krishna J

Candidate for the degree of

Master of Science

Thesis: INTENSITY MEASUREMENT OF TRAVELING WAVES IN WEBS USING LASER-DOPPLER SENSORS

Major Field: Mechanical Engineering

Biographical:

Personal Data: Born in Berhampur, Orissa, India, on August 28, 1970, the son of Sarada and Subrahmanyam Vedula.

Education: Graduated from L.D.G.Junior College, Vizianagaram, A.P., India in June 1987; received Bachelor of Technology degree in Mechanical Engineering from Bapatla Engineering College, Nagarjuna University, Bapatla, India. Completed the requirements for the Master of Science degree with a major in Mechanical Engineering at Oklahoma State University in May 1995.

Experience: Worked as a summer intern in Visakha Steel Plant, Visakhapatnam, India; performed duties as a Junior Engineer in Raymond Cements Ltd., Bhilaspur, India; employed by Oklahoma State University as a graduate research assistant; Oklahoma State University, Department of Mechanical and Aerospace Engineering, Aug. 1993 to present.

Professional Memberships: American Society of Mechanical Engineers